PHYSICAL REVIEW D **87,** 095014 (2013)

Triplet Higgs boson collider phenomenology after the LHC

Christoph Englert,[1,*] Emanuele Re,[2,†] and Michael Spannowsky[1,‡]

[1]*Department of Physics, Institute for Particle Physics Phenomenology, Durham University, Durham DH1 3LE, United Kingdom*
[2]*Department of Physics, Rudolf Peierls Centre for Theoretical Physics, University of Oxford, Oxford OX1 3NP, United Kingdom*

(Received 8 March 2013; published 23 May 2013)

ATLAS and CMS have discovered a standard model (SM) Higgs-like particle. One of the main discovery channels is the Higgs decay to two photons, which, at the moment, seems to be considerably enhanced over the standard model expectation. Models with additional charged matter coupling to the Higgs sector can enhance or decrease the $h \to \gamma\gamma$ branching ratio. We take this as motivation to confront the so-called Georgi-Machacek model of Higgs triplets with the results of recent searches for a SM Higgs boson performed at the LHC. We also investigate the model in regions of the allowed parameter space relevant for a SM-like phenomenology. The Georgi-Machacek model avoids tree-level issues of the T parameter, while offering a vastly modified Higgs phenomenology compared to the standard model. This comes at the price of introducing another fine-tuning problem related to electroweak precision measurements. We investigate the collider phenomenology of the Georgi-Machacek model in the light of existing collider constraints beyond any effective field theory approximation and contextualize our findings with electroweak precision constraints.

DOI: 10.1103/PhysRevD.87.095014 PACS numbers: 12.60.Fr, 14.80.Ec, 13.85.Rm

I. INTRODUCTION

ATLAS and CMS have reported on the discovery of a standard model (SM) Higgs-like particle [1] with a mass of approximately 126 GeV [2–5]. Bounds on production of SM Higgs-like states with heavier masses have been established as low as $\sigma \times \mathrm{Br}/[\sigma \times \mathrm{Br}]_{\mathrm{SM}} \simeq 0.1$.

In the light of the late discovery which hints at deviations from the SM expectation, attempts have been made to reconcile the excess in $h \to \gamma\gamma$ in correlation with underproduction or ''spot-on'' production in the other decay and search channels. Given that there is still consistency with the SM Higgs hypothesis within 1 to 2 sigma, these results are easily misinterpreted. Preferring one model over the other on the basis of a better χ^2 fit can be misleading: Taking the tension of the Higgs mass of 126 GeV already within the SM as an indicator of the SM's validity is certainly at odds with the tremendous success that the SM has experienced so far, culminating in the late LHC discovery.

Another way to check the validity of a certain model is to map the uncertainty of the cross sections' extraction from data onto the extended Higgs potential's parameters (and vice versa). Doing so, the SM can in principle be recovered from the Higgs sector extension for hypothetically accurate measurements without errors if the model can approach a phenomenologically well-defined decoupling limit.

An enhancement of the $h \to \gamma\gamma$ rate can typically be achieved by including additional charged states which are singlets under QCD. This predominantly alters the decay branching ratios while leaving the production cross sections unmodified apart from higher order corrections and mixing effects. Higgs triplet extensions which included color-neutral but up to doubly charged scalar particles are therefore well-motivated model-building options to reconcile the current observations [6–8]. Constraints from electroweak precision measurements and the correlation of the Higgs candidate production cross section with exclusion bounds, that are relevant for the remaining Higgs particles, are typically treated as a nuisance in this context.

In simple triplet Higgs extensions, i.e., by introducing a complex $\mathbf{3}_1$ under $\mathrm{SU}(2)_L \times \mathrm{U}(1)_Y$, the additional Higgs bosons' phenomenology in SM-like search channels is typically suppressed. This comes from the fact that their couplings to the SM fields are controlled by unitarity requirements being saturated by the 126 GeV candidate and by the small triplet's vacuum expectation value (vev) needed for consistency with the T parameter (the W/Z mass ratio) [9]. If the T parameter issue is resolved at tree level by including another real triplet Higgs field under $\mathrm{SU}(2)_L$, in what has become known as the Georgi-Machacek model [10], the Higgs phenomenology becomes more involved, and the current measurements imply nontrivial constraints on particle masses, couplings and the extended Higgs potential.

In the present paper we confront the Georgi-Machacek model of Higgs triplets [10] with the measured results from LHC Higgs searches of the 7 and 8 TeV runs. More precisely, we perform scans over a simplified version of the model's potential to identify the parameter region which is allowed in the light of current direct searches and electroweak precision measurements. Doing so, our approach is complementary to previous work by other

*christoph.englert@durham.ac.uk
†emanuele.re@physics.ox.ac.uk
‡michael.spannowsky@durham.ac.uk

groups (see, e.g., Refs. [6,8,11–14]). Instead of using an effective Lagrangian to extract information on the Higgs couplings from data and then map these constraints on the model parameter space, we use the full model and compare its predictions at a given point in the parameter space with the observed data. We also include constraints from electroweak precision measurements performed during the LEP era, thus providing (to our knowledge) the most detailed analysis of this model in the context of LEP and LHC collider measurements hitherto.

This work is organized as follows. We review the Georgi-Machacek (GM) model in Sec. II to make this paper self-contained and comprehensive. In particular we introduce the potential that we scan in the remainder of this work. In Sec. III we discuss the bounds which we take into account when scanning over the extended Higgs sector phenomenology. We also give some technical details of our implementations. Section IV is finally devoted to results, where we also detail the parameter choices of our scan. We present our conclusions in Sec. V.

II. THE MODEL

It is well known that Higgs triplets naively face compatibility issues with electroweak precision data. This is due to the fact that a simple triplet Higgs extension of the Higgs potential leads to tree-level custodial isospin violation, which is not present for complex (symplectic) $\mathrm{SU}(2)_L$ doublets accidentally (as a consequence of renormalizability and gauge invariance). This violation requires the Higgs triplet's vev to be small compared to the weak scale in order to obtain the experimentally observed m_W/m_Z mass ratio.

Reconciling the $\rho = 1 + \alpha T$ parameter (at least at tree level) in a model with triplets requires more than a single triplet field [10]. This can be seen by reminding ourselves of how custodial isospin comes about for the SM doublet Φ: If Φ transforms as a **2** under $\mathrm{SU}(2)_L$, then so does $\Phi^c = i\sigma^2\Phi^*$. Consequently, the Higgs potential depending only on $|\Phi|^2$ has a larger symmetry $\mathrm{SU}(2)_L \times \mathrm{SU}(2)_R \simeq \mathrm{SO}(4)$, which breaks to $\mathrm{SU}(2)_D$ after the Higgs obtains its vev. This ensures that the resulting electroweak gauge boson masses are related by *only* the weak mixing angle. In order to establish a $\mathrm{SU}(2)_R$ global symmetry in the Higgs potential also in presence of $\mathrm{SU}(2)_L$ triplets, we need to enlarge the field content with a real triplet such that $\mathrm{SU}(2)_R$ can act on the complex triplet, its charge-conjugated version and the real triplet.

The GM model therefore introduces the Higgs fields

$$\Phi = \begin{pmatrix} \phi_2^* & \phi_1 \\ -\phi_1^* & \phi_2 \end{pmatrix}, \qquad \Xi = \begin{pmatrix} \chi_3^* & \xi_1 & \chi_1 \\ -\chi_2^* & \xi_2 & \chi_2 \\ \chi_1^* & -\xi_1^* & \chi_3 \end{pmatrix}. \quad (1)$$

In this notation, Φ is simply a SM-like Higgs doublet and Ξ combines the complex (χ_1, χ_2, χ_3) and real $(\xi_1, \xi_2, -\xi_1^*)$ triplets. Note that while symmetry breaking with a correct ρ parameter can be fully achieved with only Ξ, the introduction of fermion mass terms still requires the presence of a SM-like Higgs doublet.

The Higgs sector Lagrangian that we consider in the remainder is

$$\mathcal{L} = \frac{1}{2}\mathrm{Tr}[D_{2,\mu}\Phi^\dagger D_2^\mu \Phi] + \frac{1}{2}\mathrm{Tr}[D_{3,\mu}\Xi^\dagger D_3^\mu \Xi] - V(\Phi, \Xi) + \Phi\,\text{Yukawa interactions}, \quad (2a)$$

with the potential

$$V(\Phi,\Xi) = \frac{\mu_2^2}{2}\mathrm{Tr}(\Phi^c\Phi) + \frac{\mu_3^2}{2}\mathrm{Tr}(\Xi^c\Xi) + \lambda_1[\mathrm{Tr}(\Phi^c\Phi)]^2 + \lambda_2\mathrm{Tr}(\Phi^c\Phi)\mathrm{Tr}(\Xi^c\Xi) + \lambda_3\mathrm{Tr}(\Xi^c\Xi\Xi^c\Xi) + \lambda_4[\mathrm{Tr}(\Xi^c\Xi)]^2 - \lambda_5\mathrm{Tr}(\Phi^c t_2^a \Phi t_2^b)\mathrm{Tr}(\Xi^c t_3^a \Xi t_3^b). \quad (2b)$$

D_2, D_3 are the covariant derivatives for the doublet and triplet representations, respectively, e.g.,

$$D_{2,\mu}\Phi = \partial_\mu\Phi + ig_w t_2^a W_\mu^a \Phi - ig_y B_\mu \Phi t_2^3. \quad (3)$$

Hypercharge $\mathrm{U}(1)_Y$ is embedded into $\mathrm{SU}(2)_R$ as in the SM. The $\mathfrak{su}(2)$ generators are $t_2^a = \sigma^a/2$ and

$$t_3^1 = \frac{1}{\sqrt{2}}\begin{pmatrix} 0 & 1 & 0 \\ 1 & 0 & 1 \\ 0 & 1 & 0 \end{pmatrix}, \qquad t_3^2 = \frac{i}{\sqrt{2}}\begin{pmatrix} 0 & -1 & 0 \\ 1 & 0 & -1 \\ 0 & 1 & 0 \end{pmatrix}, \qquad t_3^3 = \begin{pmatrix} 1 & 0 & 0 \\ 0 & 0 & 0 \\ 0 & 0 & -1 \end{pmatrix}. \quad (4)$$

The potential in Eq. (2b) is a simplified version of the allowed terms documented in Refs. [15,16]: the more general renormalizable and gauge invariant potential would allow different vevs for the two triplet fields, and would also include cubic terms [Eq. (B3) of Ref. [15]]. Terms of the former type are $\mathrm{SU}(2)_R$ violating, and we avoid them by requiring exact custodial invariance at tree level, as remarked in the following. Terms with an odd number of scalars can be easily avoided by means of a $\mathbb{Z}_2$ symmetry acting onto the triplet fields. Moreover, our analysis is only indirectly affected by the Higgs trilinear couplings (for measurement strategies of the latter see Ref. [17]), and therefore our results are general enough to assess the impact of Higgs measurements. Hence, our choice for $V(\Phi, \Xi)$ should be thought of as a minimal ansatz, that captures the important features of Higgs triplet phenomenology such as modified Higgs branching ratios, production cross sections and Higgs mixing in a well-defined way.

Switching off hypercharge gauging and the Yukawa interactions, the Lagrangian is manifestly invariant under

$SU(2)_L \times SU(2)_R$. Gauging a subgroup amounts to explicit breaking of custodial isospin, and the effects of custodial isospin violation are steered by gauge and Yukawa couplings. Hence, a small T parameter can be considered natural [18].

Electroweak symmetry breaking is triggered by the scalar fields developing vevs,

$$\langle \Phi \rangle = v_\Phi/\sqrt{2}\mathbb{1}, \qquad \langle \Xi \rangle = v_\Xi \mathbb{1}, \tag{5}$$

as a consequence of minimizing the Higgs potential which also allows us to eliminate $\mu_{2,3}^2$ and express them as functions of vevs and λ's. The vevs in Eq. (5) are in accordance with preserved custodial isospin. In principle we could have $\langle \chi_3 \rangle \neq \langle \xi_2 \rangle$, which would be induced in a $SU(2)_R$-violating potential. In the following we *impose* $SU(2)_R$ invariance and such terms are absent. This will have interesting consequences for the T parameter.

The masses of the electroweak bosons m_W, m_Z after symmetry breaking follow the usual pattern of vev $\times$ electroweak coupling, but the electroweak scale is now generated by both the doublet and the triplet vevs,

$$(246\ \text{GeV})^2 \simeq v_{\text{SM}}^2 = v_\Phi^2 + 8v_\Xi^2. \tag{6}$$

As usual, it is useful to parametrize the relative contribution of v_Φ and v_Ξ to v_{SM} via trigonometric functions:

$$\cos\theta_H =: c_H = \frac{v_\Phi}{v_{\text{SM}}}, \qquad \sin\theta_H =: s_H = \frac{2\sqrt{2}v_\Xi}{v_{\text{SM}}}. \tag{7}$$

Compared to "ordinary" complex triplet Higgs extensions, as considered recently in, e.g., Refs. [7,19] to reconcile the $h \to \gamma\gamma$ enhancement, there is no requirement to have a hierarchy $v_\Xi \ll v_\Phi$, i.e., the phenomenology of electroweak bosons can be highly different from the SM without being in immediate tree-level conflict with electroweak precision data. This is our main motivation to reinterpret the current Higgs results in the context of the GM model.

The masses that arise from expanding the extended Higgs sector around the minimum can be classified according to custodial isospin following the above remarks. Equation (2) yields a quintet, two triplets and two singlets. The massless triplet contains the longitudinal degrees of freedom of the electroweak gauge bosons, while the singlets mix as a consequence of Eq. (2b). After diagonalizing the singlet mixing of H_Φ, H_Ξ,[1]

$$H_0 = c_q H_\Phi + s_q H_\Xi, \qquad H_0' = -s_q H_\Phi + c_q H_\Xi, \tag{8}$$

the Higgs mass spectrum reads

$$\begin{aligned} m_{H_0}^2 &= 2(2\lambda_1 v_\Phi^2 + 2(\lambda_3 + 3\lambda_4)v_\Xi^2 + m_{\Phi\Xi}^2), \\ m_{H_0'}^2 &= 2(2\lambda_1 v_\Phi^2 + 2(\lambda_3 + 3\lambda_4)v_\Xi^2 - m_{\Phi\Xi}^2), \\ m_{H_3}^2 &= \frac{1}{2}\lambda_5(v_\Phi^2 + 8v_\Xi^2), \qquad m_{H_5}^2 = \frac{3}{2}\lambda_5 v_\Phi^2 + 8\lambda_3 v_\Xi^2, \end{aligned} \tag{9}$$

where

$$\begin{aligned} m_{\Phi\Xi}^2 = [&4\lambda_1^2 v_\Phi^4 - 8\lambda_1(\lambda_3 + 3\lambda_4)v_\Phi^2 v_\Xi^2 \\ &+ v_\Xi^2(3(2\lambda_2 - \lambda_5)^2 v_\Phi^2 + 4(\lambda_3 + 3\lambda_4)^2 v_\Xi^2)]^{1/2}, \end{aligned} \tag{10}$$

and

$$\sin\angle(H_\Phi, H_0) =: s_q = \frac{\sqrt{3}}{\sqrt{3 + \left[\frac{2\lambda_1 v_\Phi^2 - 2(\lambda_3+3\lambda_4)v_\Xi^2 + m_{\Phi\Xi}^2}{(2\lambda_2 - \lambda_5)v_\Phi v_\Xi}\right]^2}}. \tag{11}$$

Note that the model contains a $\mathcal{CP}$ odd scalar H_3^0 which is the neutral component of the massive custodial triplet (more precisely, the $\mathcal{CP}$ odd scalar is the non-Z_L combination of $\Im\{\phi_2\}$ and $\Im\{\chi_3\}$).

Writing the full Lagrangian in terms of the mass eigenstates we recover the Feynman rules of the theory. For a general gauge (i.e., including the Goldstone sector) we find $\mathcal{O}(500)$ potentially nonzero interaction vertices—obviously too many to discuss here. Most of the Feynman rules, however, arise from the Higgs sector including the Higgs self couplings, Eq. (2b). We have computed the Feynman rules using FEYNRULES [20] and validated the output against an in-house Feynman rule extraction code. Some of the Feynman rules can be found in earlier publications [6,11,12,15,16,21] and we also have performed analytical comparisons with these results.[2]

Before we discuss the bounds which we take into account for the results of Sec. IV let us foreclose some characteristic properties of the GM model Eqs. (1)–(11):

(1) In contrast to models with a doublet and one complex triplet only, the GM model *a priori* allows for sizable triplet vevs. Therefore, the couplings of the neutral Higgs mass eigenstates (in particular the two custodial singlets H_0 and H_0') can highly differ from the SM Higgs couplings. We denote the universal ratios of the hVV and $hf\bar{f}$ couplings of H_0, H_0' with respect to the SM values by

[1] $H_\Phi \sim \Re\{\phi_2\}$ whereas H_Ξ is the linear combination of ξ_2 and $\Re\{\chi_3\}$ which yields a custodial singlet.

[2] In particular, to recover the Feynman rules for the Higgs self couplings listed in [16], we notice that the λ's couplings of [16] can be obtained from ours with the substitutions $\lambda_1 \to \lambda_1 + \lambda_3$, $\lambda_2 \to 2\lambda_3 + \lambda_4$, $\lambda_3 \to 3\lambda_5$, $\lambda_4 \to \lambda_2 + \lambda_3 - \lambda_5$, $\lambda_5 \to 2\lambda_4$. A number of Feynman rules in the GM phenomenology-pioneering work of Ref. [16] have been superseded in Ref. [6].

$$c_{t,H_0} = \frac{c_q}{c_H}, \quad c_{v,H_0} = c_q c_H + \sqrt{8/3} s_q s_H,$$
$$c_{t,H_0'} = -\frac{s_q}{c_H}, \quad c_{v,H_0'} = -s_q c_H + \sqrt{8/3} c_q s_H. \tag{12}$$

The above equations show that c_v can be larger than unity, a typical property of models with weak isospin $j > 1/2$ multiplets [22]. It is interesting to observe from the above expressions that values $|c_v| > 1$ are possible only when the term with the prefactor $\sqrt{8/3} \sim 1.6$ dominates over the first term. Values of $|c_v|$ very close to one can be obtained either when the first term is very close to unity (which means very small triplet vev and minimal mixing in the singlet sector, i.e., c_q very close to one or zero) or when there is a compensation between the two terms in $|c_v|$. This compensation can potentially take place only when the second term is not too suppressed, i.e., an enhanced $|c_v|$ does not occur for $0 \leq s_H \ll 1$.

(2) Another very interesting feature of the GM model shows up for vanishing mixing of the singlet states. In this situation the mass eigenstates are by definition aligned with the H_Φ, H_Ξ states. If we take the limit $s_H(c_H) \simeq 0$, which corresponds to breaking electroweak symmetry mainly with the doublet (triplet) vev, we get a massless scalar in the spectrum. This state always corresponds to H_0' and, as we will see, it has important consequences for the model's phenomenology.

Away from the edges of the parameter space (i.e., when neither s_H nor c_H are very small, and λ's are all of the same order), the above mechanism can be rephrased by saying that the lighter custodial singlet Higgs boson is usually the one which is less related to electroweak symmetry breaking [16]. When the mixing in the singlets sector is non-negligible, the mass spectrum becomes effectively less affected by this property, and the mass of the lightest Higgs boson can be made sizable: the allowed size of this misalignment is encoded in our results.

Moreover, despite these considerations, all states clearly contribute to unitarization of longitudinal gauge boson scattering (the longitudinal gauge bosons are mixtures of the triplet Ξ and doublet Φ), and this has interesting implications for the electroweak precision constraints, especially in the scenario discussed in Sec. IV A.

For a more general potential that also violates $SU(2)_R$ invariance, the $s_H \to 0$ limit does not necessarily involve $m_{H_0'} \to 0$, cf. [15]. For these more general potentials there always exist parameter choices that involve light scalars in the spectrum. The correlation with s_H, however, is not so obvious. Generically the light scalars follow from parameters with a small $SU(2)_R$ breaking. Since $\rho \simeq 1$ is well established experimentally, invariance under global $SU(2)_R$ is well established too, and the allowed isospin violation can be treated as a perturbation which should restore, to large extent, the correlation between vanishing s_H and $m_{H_0'} \to 0$, for phenomenologically allowed choices. In fact, the limit $v_\Xi \to 0$ in Eq. (2b) is tantamount to $\mu_3^2 \to (-2\lambda_2 + \lambda_5) v_{\rm SM}^2$, which means that the custodial singlet part of the Higgs potential effectively "sees" a vanishing mass term, while this is not the case for the custodial triplet and quintet.

III. BOUNDS

The implications of the GM model for the Peskin-Takeuchi S, T, U parameters [9],

$$S = \frac{4 s_w^2 c_w^2}{\alpha}\left(\frac{\Pi_{ZZ}(m_Z^2) - \Pi_{ZZ}(0)}{m_Z^2} - \frac{c_w^2 - s_w^2}{c_w s_w}\frac{\Pi_{AZ}(m_Z^2) - \Pi_{AZ}(0)}{m_Z^2} - \frac{\Pi_{AA}(m_Z^2) - \Pi_{AA}(0)}{m_Z^2}\right),$$
$$T = \frac{1}{\alpha}\left(\frac{\Pi_{WW}(0)}{m_W^2} - \frac{\Pi_{ZZ}(0)}{m_Z^2} - \frac{2 s_w}{c_w}\frac{\Pi_{AZ}(0)}{m_z^2} - \frac{s_w^2}{c_w^2}\frac{\Pi_{AA}(0)}{m_Z^2}\right),$$
$$U = \frac{4 s_w^2}{\alpha}\left(\frac{\Pi_{WW}(m_W^2) - \Pi_{WW}(0)}{m_W^2} - c_w^2\frac{\Pi_{ZZ}(m_Z^2) - \Pi_{ZZ}(0)}{m_Z^2} - s_w^2\frac{\Pi_{AA}(m_Z^2) - \Pi_{AA}(0)}{m_Z^2} - 2 s_w c_w \frac{\Pi_{AZ}(m_Z^2) - \Pi_{AZ}(0)}{m_Z^2}\right), \tag{13}$$

have been pioneered in Ref. [23].

The parameters Π_{XY} denote the gauge boson polarization functions which are obtained from the two-point functions $X \to Y$ ($X, Y = A, Z, W$),

$\Pi_{XY}(Q^2) \sim$ 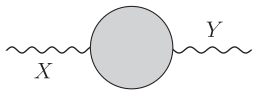 , (14)

α is the fine structure constant and s_w, c_w are the sine and cosine of the weak mixing angle as usual. The blob denotes all particle dynamics which enters the polarization functions in the corresponding model.

At this stage, it is important to note a peculiarity of the T parameter that arises in the tree-level $SU(2)_R$ symmetric GM model. Although the identification between the real and complex triplets' vevs yields the correct tree-level W/Z mass ratio, the situation becomes more involved at the one-loop. The real triplet's vev requires the introduction of a counterterm (related to the weak mixing angle renormalization) that could be naively unexpected from the $SU(2)_R$-symmetric tree-level Lagrangian [23]. This counterterm mends a residual UV singularity in the T parameter. In this sense, $SU(2)_R$ invariance introduces an additional naturalness problem in addition to the conventional hierarchy problem, namely why the T parameter remains small. This finding is somewhat similar to the original T parameter problem in $SU(2)_R$-violating triplet extensions.

Performing the full one-loop calculation with the Feynman rules described in the previous section, we find that, after introducing a corresponding T parameter counterterm, our calculation is manifestly free of UV divergencies; no residual UV divergencies appear in neither the S nor in the U parameter, in accordance with the results of Ref. [23].

As pointed out in Ref. [23], the GM model picks up a quadratic T parameter divergence which introduces a fine-tuning problem analogous to the Higgs mass. The T parameter constraint is very stringent and will probe the finite logarithms. If these logarithms are of order one, a large one-loop T parameter can decrease again when the full perturbative expansion is known.[3] We therefore trace the effect of imposing S independent from T in Sec. IV. When imposing only the S parameter constraint we set $T = 0$. This can in principle be interpreted as a situation where a large T shows up as relic of perturbation theory.

At this point it is worthwhile to comment on the applicability of S, T, U for the present model. Estimating new physics effects by means of S, T, U assumes, among other approximations [25], that the new physics scale Λ is larger than m_Z. Identifying m_{H_0} as the 126 GeV candidate we can face spectra for which $m_{H_0'}$ is close to or even below the Z threshold. In this case, the expansion of the vacuum polarization functions in terms of Q^2/Λ^2 on which S, T, U rely[4] could be ill-defined if the coupling $|c_{v,H_0'}|$ is large. Then, the light scalar cannot be considered a small perturbation compared to the heavier states' impact. Including the LEP constraints on light SM-like Higgs production ($m_H \leq 114$ GeV), which probe combined mixings down to $c_v^2 \sim 0.01$, the S, T, U bounds are superseded by the direct exclusion from $e^+e^- \to hZ$ searches. If the mixing is too large, the direct LEP constraints remove the parameter point from the list of valid points, especially when the resulting ΔS falls into the allowed region, and our theoretical predicament is resolved phenomenologically.

Additional constraints that in principle reduce the model's allowed parameter space follow from nonoblique corrections, e.g., corrections the $Zb\bar{b}$ vertex, and flavor physics. Modifications of the flavor sector are induced by "rotating in" the custodial triplet (H_3^+, H_3^0, H_3^-) via Goldstone mixings in the extended space of Higgs fields, Eq. (1), and by the singlets' mixing.

These mixings are parametrically controlled by c_q, s_q, c_H and s_H. The qualitative modifications in the flavor sector in comparison to the SM are similar to a two-Higgs doublet model without flavor changing neutral currents [26]. We expect that consistency with flavor constraints can be achieved without too large quantitative changes induced (see, e.g., Ref. [8]). Especially for scenarios with tuned T, which, as we will see in Sec. IV, are consistent for small s_H, we can expect flavor physics to be SM-like. Similar arguments hold for the nonoblique corrections, e.g., the $Zb\bar{b}$ vertex does not receive corrections from the quintet states at the one-loop level [27].

Beyond indirect constraints such as electroweak precision measurements, there are already direct constraints from searches $H_5^{\pm\pm} \to \ell^\pm\ell^\pm$ ($\ell = e, \mu$) by both ATLAS and CMS [28]. Such a decay can be prompt by the introduction of a Majorana-type interaction term of the triplet and the leptons and constrains a different sector of the model. The bounds of Ref. [28] assume coupling strengths of order 1 to derive lower mass limits on the quintet mass. While this assumption is reasonable to obtain a well-defined limit in hypothesis tests, especially for a heavy quintet $m_{H_5} \gtrsim 2m_W$ this is not reasonable. For large m_{H_5}, we need to include a partial decay width which is dominated by longitudinally polarized W bosons. This leads to a tree-level dependence of the partial decay width $\Gamma(H_5^{\pm\pm} \to W^\pm W^\pm) \sim m_{H_5}^3/m_W^2$. Just like in the SM, the decay to light fermions scales $\Gamma(H_5^{\pm\pm} \to \ell^\pm\ell^\pm) \sim m_{H_5}$, and the decay to same-sign leptons quickly becomes subdominant. Searches for same-sign inclusive dileptons exist [29] but are typically designed to cope with nonresonant squark-gluino production [29,30]. Additional constraints from leptonic final states can be obtained from measurements of lepton flavor violating $\mu^\pm \to e^+e^-e^\pm$ [31–33].

We do not include these constraints in detail in the following. We however note that dedicated limits can be obtained from an analysis of the $\ell^\pm\ell^\pm jj$ final state for $H_5^{\pm\pm}$ production via weak boson fusion (WBF).

IV. RESULTS

We now turn to the results of our scans over the Higgs potential. The role of the Higgs candidate can in principle be played by all uncharged Higgs states H_0, H_0', H_3^0, H_5^0. In the light of recent results, however, it is unreasonable to study H_3^0 and H_5^0 in further detail:

(i) H_3^0 is a $\mathcal{CP}$ odd state which does not couple to the massive vector bosons. The measurement of the Higgs candidate in the ZZ channel [2,3] which also disfavors pure $\mathcal{CP}$ odd quantum numbers from angular distributions in the leptonic decay channels [34] removes H_3^0 from our list of candidates. Note that constraints on $\mathcal{CP}$ odd scalars directly constrain λ_5, Eq. (9). Furthermore, a 126 GeV H_3^0 is also disfavored from flavor physics and nonoblique corrections [27].

(ii) Even though H_5^0 has the right quantum numbers and vertex structures to mimic the branchings to the $\gamma\gamma$, ZZ and WW final states, the quintet is fermiophobic

[3] See, e.g., Ref. [24] for a solution to the Higgs naturalness problem in this context.

[4] We would like to remind the reader that small allowed S, T, U values are necessary but not sufficient conditions for consistency with electroweak precision data. The latter requires carrying out an analysis including model-dependent radiative corrections to at least next-to leading order.

as a consequence of the $SU(2)_R$ symmetry. This removes gluon fusion [35] as production mode and leaves inclusive weak boson fusion [36] as the largest production cross section for H_5^0. Weak boson fusion for inclusive cuts is typically suppressed by 1 order of magnitude compared to gluon fusion [37]. Reconciling the measurements in ZZ, WW, $\gamma\gamma$, $\tau^+\tau^-$ with the observed rates is therefore impossible, and H_5^0 cannot play the role of the 126 GeV candidate, when considering recent limits on the total Higgs width [38].

From Eq. (9) it is manifest that H_0' is always lighter than H_0, and hence H_0' is the natural candidate to play the role of the observed Higgs. As already mentioned in Sec. III, we will also study the scenario where there is a lighter uncharged scalar state in the mass spectrum, which we can achieve by fixing $m_{H_0} = 126$ GeV. However, we will see that this scenario is disfavored.

Although partial motivation of this work is to explore the GM model's potential to enhance the $h \to \gamma\gamma$ branching ratio via the presence of extra matter, it is clear from the Higgs couplings not fixed to the SM values [Eq. (12)] that the $\gamma\gamma$ branching ratio in this model is also affected by these modified tree-level couplings. This means that it is indeed possible to find regions in the parameter space where $\mathrm{Br}(H \to \gamma\gamma)$ is very close to the SM also without forcing the charged Higgses to be very heavy. We will briefly explore this possibility too, by looking for points that reproduce the Higgs signal and at the same time have a $\gamma\gamma$ branching ratio close to unity. Precise fits on Higgs couplings will eventually tell whether this is a feasible scenario, although recent studies by several collaborations favor regions with $|c_t|, |c_v| \sim 1$.

The cross section limits for the uncharged Higgs fields are adopted from the most recent LHC measurements [4,5] and from the combined LEP constraints [39]. In particular for Higgs masses smaller than the LEP direct bound, we use the LEP bound on the HZZ coupling.

Signal strengths are defined as follows:

$$\mu_{h\to XX} = \frac{\sigma(pp \to h) \times \mathrm{Br}(h \to XX)}{\sigma_{\mathrm{SM}}(pp \to h) \times \mathrm{Br}_{\mathrm{SM}}(h \to XX)}, \tag{15}$$

and for this paper we define the combined signal strength as

$$\mu_h = \frac{\sigma(pp \to h) \times [\mathrm{Br}(h \to WW) + \mathrm{Br}(h \to ZZ) + \mathrm{Br}(h \to \gamma\gamma)]}{\sigma_{\mathrm{SM}}(pp \to h) \times [\mathrm{Br}_{\mathrm{SM}}(h \to WW) + \mathrm{Br}_{\mathrm{SM}}(h \to ZZ) + \mathrm{Br}_{\mathrm{SM}}(h \to \gamma\gamma)]} \tag{16}$$

since ATLAS and CMS use the categories WW, ZZ, $\gamma\gamma$, $\tau\tau$ and $Vb\bar{b}$ to obtain the exclusion bounds from data, and the latter two categories give a marginal contribution to μ_h, because of nonobservation of the Higgs and large experimental errors in those channels. Equation (16) does not take into account the different channels' sensitivity which is beyond the scope of this work.

We scan $\lambda_i \in [-4\pi, 4\pi]$, $i = 1, \ldots, 5$ and $s_H \in [0, 1]$, which also implies that since λ_5 is bounded from above, in our scan the maximum value allowed for m_{H_3} is $\sim$600 GeV. To generate parameter points with $m_{H_0'}(m_{H_0}) = 126 \pm 1$ GeV more efficiently, we first generate the mass of the 126 GeV state, and then compute λ_1 (λ_1 and λ_2) using Eq. (9). The generated parameter points are, hence, not flat and should by no means be understood as probability distributions of parameter points that pass the requirements.

All the LHC measurements of the Higgs-candidate properties, in particular from the WW, ZZ and $\gamma\gamma$ categories, point towards a Higgs phenomenology with $|c_t|$ and $|c_v|$ not dramatically different from the SM values [8,40,41]. Moreover, the combined signal strengths from CMS and ATLAS are $\mu_{h,\mathrm{CMS}} \simeq 0.9 \pm 0.2$ [5] and $\mu_{h,\mathrm{ATLAS}} \simeq 1.3 \pm 0.3$ [4]. We will take the ATLAS measurement as the paradigm of an enhanced $h \to \gamma\gamma$ production rate, but will also comment on the model's capability to reproduce the consistency with the SM as observed by CMS.

Since the theoretical expectation for these values is dominated by $\mu_{h\to WW} \sim |c_t c_v|^2$, it is reasonable to restrict our scans to the regions where both $|c_t|$ and $|c_v|$ are larger than 0.8.[5] Unless otherwise stated, all results have been obtained with the aforementioned condition explicitly imposed.

We use the exclusion contours by ATLAS[6] [2]. In order to reproduce the observed LHC discovery signal we need an excess of $\sim$25% for the total signal strength compared to the SM hypothesis. We therefore typically need either $|c_t|$ or $|c_v| > 1$. The cross section in the discovery channels scales as c_t^2 and the VV branching ratios as $\sim c_v^2/c_t^2$. Therefore c_t is typically less constrained in our scan, also because no statistically significant observation in the fermionic channels has been made so far. The approximate scaling for the VV branching ratio mentioned above follows from the observed "SM-likeness" of the 126 GeV Higgs boson, which in turn implies the decay to bottom quarks to be the dominant contribution to the total decay width. Notice however that in our approach we have taken into account all the possible changes to the Higgses' total

[5]The $\gamma\gamma$ excess, although phenomenologically very important if confirmed, cannot be responsible for a 20% enhancement of the global μ_h value, being a potentially large effect in a rare branching ratio.

[6]While the exclusion limits of both ATLAS and CMS do not coincide at face value, they quantitatively follow the same pattern.

widths due to non-SM-like couplings and to the extended Higgs sector. In the scenario with an uncharged scalar lighter than the 126 GeV state, a too large deviation of the total width when $H_0 \to H_0' H_0'$ opens up is limited by the experimental observation of the individual signal strengths being in good agreement with the SM values.

To estimate the signal strengths for H_0, H_0' and H_3^0 and compare with the exclusion bounds, we need their production cross sections and branching ratios. The branching ratios and total widths have been obtained interfacing FEYNRULES with a modified version BRIDGE [42], where we included the loop functions needed to evaluate the amplitudes $h \to \gamma\gamma$ via scalar, fermionic and vectorial loops. We have also included the more important QCD corrections to the $h \to b\bar{b}$, $h \to c\bar{c}$ and $h \to gg$ decays [43], and cross-checked the implementation against the SM partial widths quoted in [37]. BRIDGE also computes the branching ratios for off-shell decays.

The leading-order inclusive cross sections $\sigma(gg \to h)$ have been computed using an adapted version of the POWHEG-BOX program [44]. Using LO cross sections is a good approximation since higher order QCD corrections play a minor role as far as signal strengths are concerned. In doing so, we have also neglected the contribution from Higgs production via WBF, which plays a subleading role in our study. We leave a detailed discussion of the GM's WBF phenomenology to the future.

To impose our electroweak precision criteria we use the $S, T, (U \equiv 0)$ fits at 95% confidence level of Ref. [45].[7] We classify a point in the parameter space as "good" with respect to the m_{H_0}, $m_{H_0'} \simeq 126$ GeV triplet hypotheses according to three main different requirements as already alluded to before.

(i) *loose electroweak precision*: S within the 95% C.L. ellipse, no constraint on T. We understand this case as $T \equiv 0$, along the lines of Sec. III.

(ii) *enforced electroweak precision*: Both S, T strictly in the 95% C.L. ellipse.

(iii) *bounds from global direct searches and tagged categories*: in this case we reproduce the μ_h value for the Higgs signal within the quoted error of $\simeq 25\%$ and we do not violate the exclusion bounds for the other neutral Higgses. We also reproduce $\mu_{h\to WW}$ and $\mu_{h\to\gamma\gamma}$ within the 1σ error band.

For later convenience, we also introduce the quantity

$$c_\Xi = \begin{cases} \langle H_0' | H_\Xi \rangle = c_q, & \text{if } m_{H_0'} \simeq 126 \text{ GeV} \\ \langle H_0 | H_\Xi \rangle = s_q, & \text{if } m_{H_0} \simeq 126 \text{ GeV} \end{cases} \quad (17)$$

to quantify the overlap between the 126 GeV mass eigenstate and H_Ξ, the singlet whose mass would only be generated by v_Ξ if there was no mixing.

At this point we also note that with the conventions used in this work c_t is always negative, whereas c_v does not have a constrained sign. Although being different to the conventions often used by other groups, this is a perfectly legitimate choice that covers the physically relevant cases. As a consequence, the SM-like situation where the hVV and $hf\bar{f}$ couplings have the same sign is recovered in this work when $(c_t, c_v) = (-1, -1)$.

A. $m_{H_0} \simeq 126$ GeV—Inverted mass hierarchy

We first investigate the scenario where the Higgs candidate is more closely related to the SM Higgs doublet, i.e., $m_{H_0} \simeq 126$ GeV. This will also provide us the munition for the phenomenologically more appealing case $m_{H_0'} \simeq 126$ GeV, for which there are no constraints from Higgs decays to light states with coupling strengths of the order of the weak scale.

The scenario with $m_{H_0} \simeq 126$ GeV corresponds to a situation which should be naively similar to the SM, because we expect that on average $m_{H_0} \simeq 126$ GeV can be easily obtained when the triplet vev is small, i.e., when electroweak symmetry is mainly broken by the doublet. However, as we mentioned above, in this scenario we have $m_{H_0'}$ smaller than m_{H_0}, which obviously implies peculiar consequences on the allowed phenomenology.

Figure 1 shows the model's couplings spans in the $m_{H_0} \simeq 126$ GeV scenario, and in particular the allowed enlarged range for c_t and c_v described by Eq. (12). We start our walk through the constraints for $m_{H_0} \simeq 126$ GeV in Fig. 2, where no constraints have been imposed and the isocontours for $|c_{v,H_0}|$ and $|c_{t,H_0}|$ are shown in the (c_Ξ, s_H) plane. In Fig. 3 we impose the S parameter constraint and in the panels of Fig. 4 we further include the signal strengths of ATLAS. These steps sketch the transition from LEP to the combined Higgs discovery and exclusion.

As expected, due to $m_{H_0'} \leq m_{H_0}$, we find large deviations from the SM Higgs decay phenomenology, which is reproduced within $\simeq 2\sigma$ by the current data. In particular, we find that this feature holds even when we relax the constraints on the T parameter: for negative c_v values, $|c_v|$ is always smaller than 1, in particular when $|c_t|$ is different from 1. This can be understood from the comments after Eq. (12): indeed, in this scenario, s_H is usually relatively small, whereas $c_\Xi \sim 0$, i.e., $|c_q| \sim 1$. This means that there is room for c_t to vary around the central value (remaining however close to -1), whereas the vector coupling essentially follows from $c_q c_H$. Therefore, $|c_v|$ is bound to be smaller than 1. In particular, the more c_t deviates to -1, the smaller $|c_v|$ becomes. In such a situation, it is almost impossible to reproduce the Higgs signal: we typically find values $\mu_h \simeq 0.8$, whereas the value preferred by the

[7] During the course of this work, these fits have been updated including the Higgs measurements [46]. The differences compared to Ref. [45] are quantitatively small and not relevant for our results.

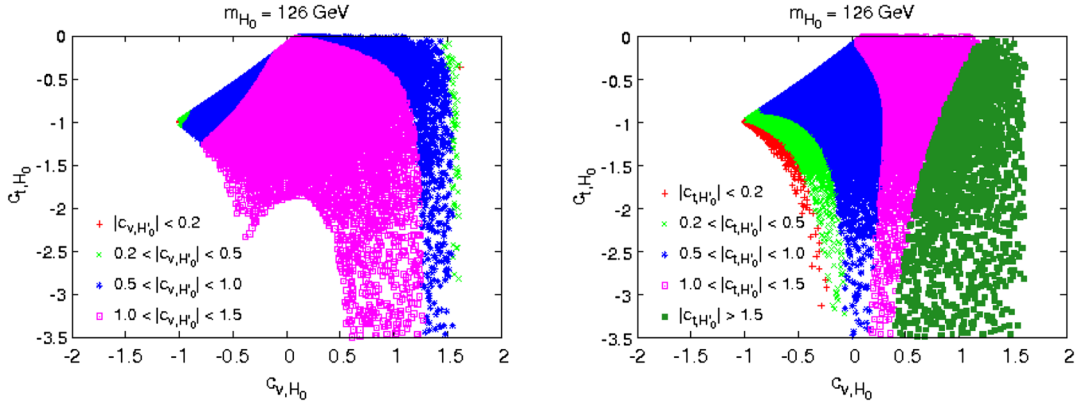

FIG. 1 (color online). (c_{v,H_0}, c_{t,H_0}) correlation for $m_{H_0} \simeq 126$ GeV. We do not impose any other additional constraint.

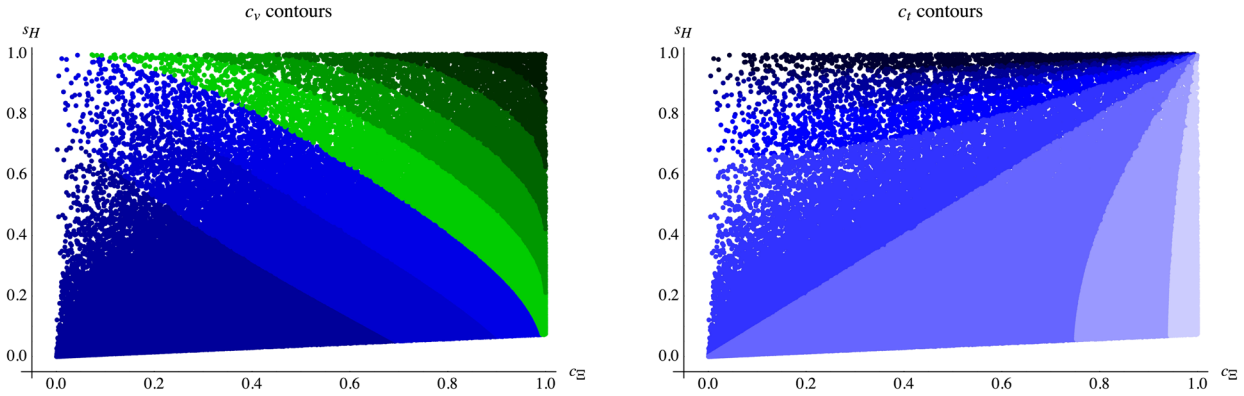

FIG. 2 (color online). Scan over the GM model's parameter space only requiring $m_{H_0} \simeq 126$ GeV in the (c_Ξ, s_H) plane. The left panel shows c_{v,H_0} contours with the following color codes: dark blue $-1 < c_v < -0.66$, dark green $1.33 < c_v < \sqrt{8/3}$. The right panel shows c_{t,H_0} contours with dark blue $c_t < -3$, light blue $-0.33 < c_t < 0$.

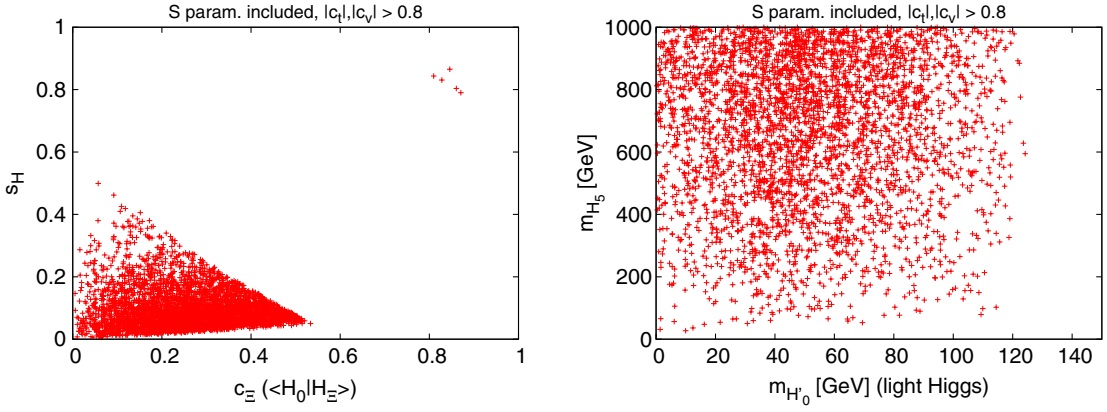

FIG. 3 (color online). Scan of Fig. 2, including precision constraints on the S parameter.

excess observed by ATLAS is $\simeq 1.25$. The few surviving points shown in Fig. 4 correspond to $\mu_h \simeq 1$, which is just within the 1σ error bar of the ATLAS global μ value. We also notice from the right plot in Fig. 4 that for all these points the decay $H_0 \to H_0' H_0'$ is closed. On the other hand, this means that a possible future decrease in the observed $h \to \gamma\gamma$ rate can in principle be accommodated by the GM triplet model in this scenario, at the price of some tension with electroweak precision measurements.

Since the only constraint we have required is the S parameter along the lines of the previous section, it is natural to think that by relaxing the S parameter condition

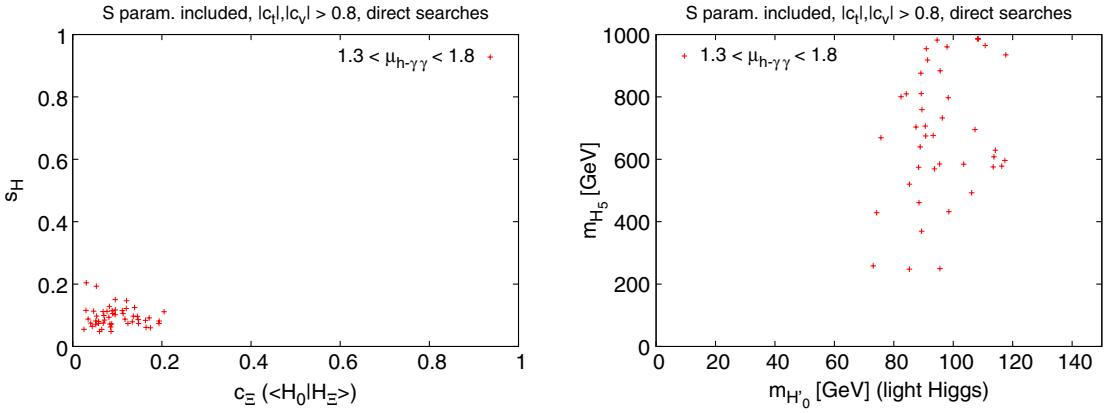

FIG. 4 (color online). Scan of Fig. 2, including precision constraints on the S parameter and signal strength constraints from direct searches.

to 99% confidence level, we can find points in the parameter space with values of c_t and c_v that allow one to reproduce the Higgs signal. Indeed, we observe that there are points with larger values of c_t and c_v that survive the relaxed electroweak precision constraints. They typically imply larger values of s_H and c_Ξ values not necessarily close to 0. Direct search constraints, however, both from LHC and LEP, remove these points, typically because they violate the LEP bound on the HZZ coupling for the light Higgs state, as can be readily seen from the left plot of Fig. 1: values of $c_{v,H_0} \geq 1$ correspond to values of $|c_{v,H_0'}|$ that are too large to survive LEP bounds.

This scenario seems to be heavily constrained by the S, T, U parameters on top of the phenomenological requirements for the observed signal strengths. The latter is expected from our previous remarks on dominant decays to the lighter Higgs states, however, one might naively expect that electroweak precision should not be too constraining as this is definitely not the case for the model's limit of the SM Higgs doublet with $m_h \simeq 126$ GeV [45]. So what is the reason for electroweak precision observables being so different from the SM in this case?

Let us step back and investigate how electroweak precision observables are qualitatively influenced in the GM model. In comparison to the SM the electroweak precision observables are influenced by the modified Higgs sector. The gauge interactions of the fermions are unchanged and by comparing to the SM reference point to calculate ΔS, ΔT, ΔU drop out. To understand the Higgs-gauge boson interactions which drive these observables via Eq. (14), it is quite instrumental to understand how unitarity conservation is realized in longitudinal gauge boson scattering in the GM model. Looking at, e.g., $W_L W_L$ scattering, a necessary condition for unitarity to be conserved in any perturbative model is that the coherent sum of new physics contributions to $WW \to WW$ has to reproduce the SM Higgs contribution for high enough energies (above all contributing thresholds). The s- and t-channel SM Higgs exchange cancels the residual amplitudes growth proportional to the W's energy squared in a minimal fashion. In the GM model this is realized more intricately as, e.g., in models with just simple Higgs mixing. While in the latter case, for high enough energies, the SM Higgs contribution is reproduced via $\sin^2\alpha + \cos^2\alpha = 1$ (α is the mixing angle), in the GM model we can have a very large enhancement of c_v by all uncharged Higgs particles to begin with. Their "over-contribution" is canceled by t- and u-channel exchange of the $H_5^{\pm\pm}$ which in the high energy limit becomes equivalent to an s-channel contribution [16]. Note that all Higgs exchange diagrams are proportional to the squared real Higgs couplings and the compensation results from kinematics t, $u \sim -s$. The two-point functions of Eq. (14) obviously do not encode any kinematics and are a coherent sum of the quartic Higgs couplings and the trilinear couplings squared. Spontaneously broken gauge invariance, on the other hand, guarantees the absence of UV singularities via cancellations among the different contributing diagrams (and the corresponding T parameter counterterm).

From Fig. 5 we can therefore immediately read off the potential issue of the GM model that arises when it is

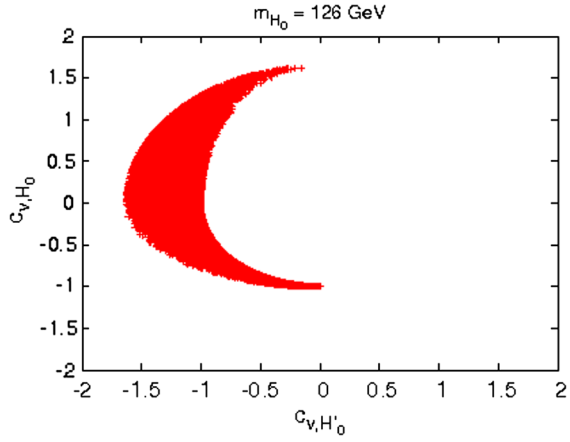

FIG. 5 (color online). $(c_{v,H_0'}, c_{v,H_0})$ for $m_{H_0} \simeq 126$ GeV. We impose neither electroweak precision constraints nor bounds from the signal strengths.

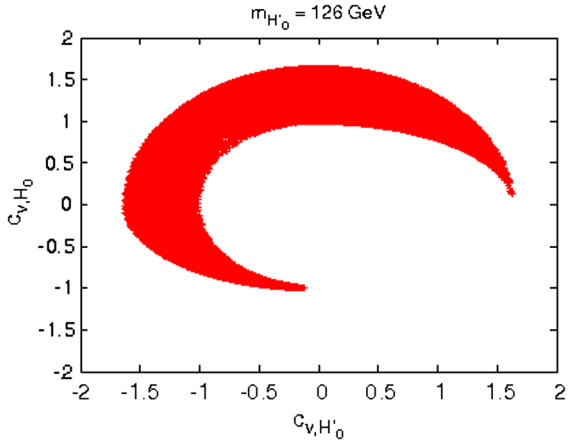

FIG. 6 (color online). $(c_{v,H_0'}, c_{v,H_0})$ for $m_{H_0'} \simeq 126$ GeV. We impose neither electroweak precision constraints nor bounds from the signal strengths.

confronted with electroweak precision measurements for $m_{H_0} \simeq 126$ GeV. There we plot the $(c_{v,H_0'}, c_{v,H_0})$ correlation for our scan with the requirement of H_0 being the observed Higgs-like candidate. Obviously there is no anticorrelation of the two Higgs states. When enforcing the observed data's constraint on $|c_{v,H_0}| \simeq 1$ (horizontal lines in Fig. 5) we typically have sizable values for $c_{v,H_0'}$: therefore ΔS generically turns out to be large when we require the Higgs candidate's couplings to reproduce the SM or to obtain even larger couplings than the SM, $c_{v,H_0} \gtrsim 1$. This together with the large deviation of the Higgs phenomenology driven by $\mathrm{BR}(H_0 \to H_0' H_0')$ highly constrains $m_{H_0} \simeq 126$ GeV, independent of a possible excess in $\mathrm{BR}(H_0 \to \gamma\gamma)$.

B. $m_{H_0'} \simeq 126$ GeV—Normal mass hierarchy

We turn to identifying H_0' with the observed Higgs candidate. In Fig. 7 we plot the different contour regions for c_{v,H_0} and c_{t,H_0} as functions of $(c_{v,H_0'}, c_{t,H_0'})$ without imposing any constraints apart from $m_{H_0'} \simeq 126$ GeV. The left-out region inside the blue contours stems from parameter points that do not give rise to (local) minimum of the potential. The model clearly predicts large enhancements of the vectorial couplings, which also manifest in an enhanced partial decay width $\Gamma(H_0' \to \gamma\gamma)$, which is a function of basic contributions: the W loop, the fermion loops and the charged scalar loops. In the SM the W loop dominates over the top contributions. Figure 7 indicates that this correlation is already significantly altered via Eq. (12): the top loop can be suppressed while the W loop is enhanced. This needs to be contrasted to ordinary complex triplet models, where, due to the small triplet vev, such an enhancement via c_v is not present and possible branching ratio enhancements need to be driven essentially only by the additional charged scalars.

The contribution from, e.g., charged $H_5^\pm$ and $H_5^{\pm\pm}$ scalars in the GM model to the $H_0' \to \gamma\gamma$ amplitude scales as $F(s_H, \vec{\lambda}) Q_{h_5}^2 [v_{\mathrm{SM}}^2/(2m_5^2)] A_0(m_{H_0'}^2/4m_{H_5}^2)$, where F is a function of the parameter space and A_0 is the typical one-loop 3-point function encountered in such amplitudes [35]. A similar relation holds for $H_3^\pm$. The 3-point function is essentially constant for masses larger than $m_{H_5} \gtrsim 200$ GeV, $A_0 \simeq 0.35$. In the end the charged scalar effect can be compensated by the vast parameter range that is admissible due to changes in (c_v, c_t), which can also constructively interfere as a consequence of Eq. (12). We find that the H_5 contribution is typically small and destructive over the parameter range that we consider, i.e., it works against the W contribution; this means that a necessary condition to have $\mathrm{BR}(H_0' \to \gamma\gamma) \gtrsim \mathrm{BR}(H_0' \to \gamma\gamma)_{\mathrm{SM}}$ is that the destructive interference of the SM t and $W^\pm$ is reduced or becomes constructive.

We again start our walk through the constraints for $m_{H_0'} \simeq 126$ GeV in Fig. 8. In Fig. 9 we impose the S parameter constraint and in the panels of Fig. 10 we include the signal strengths of ATLAS. We show the fully tuned setup in the analogous Figs. 11 and 12. From Fig. 6 we expect the $m_{H_0'} \simeq 126$ GeV scenario to be less sensitive

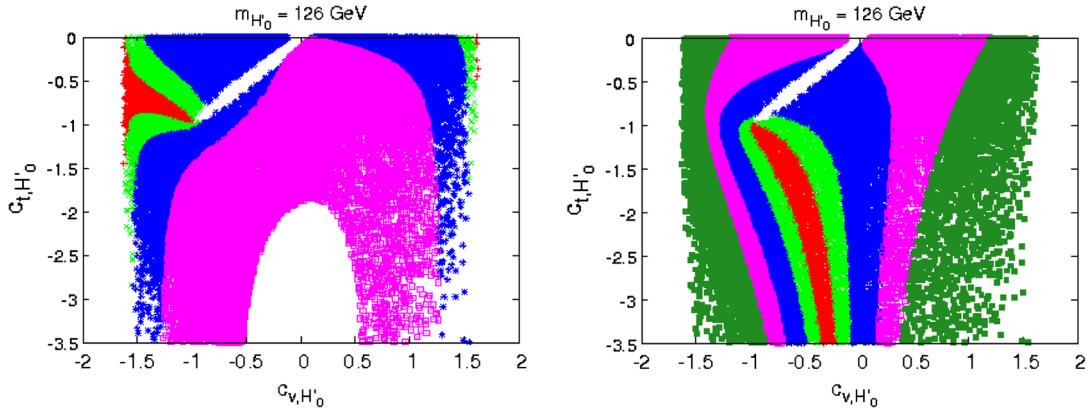

FIG. 7 (color online). $(c_{v,H_0'}, c_{t,H_0'})$ correlation for $m_{H_0'} \simeq 126$ GeV. We do not impose any other additional constraints. The color code is the same as in Fig. 1, although here contours are for c_{v,H_0} (on the left panel) and c_{t,H_0}.

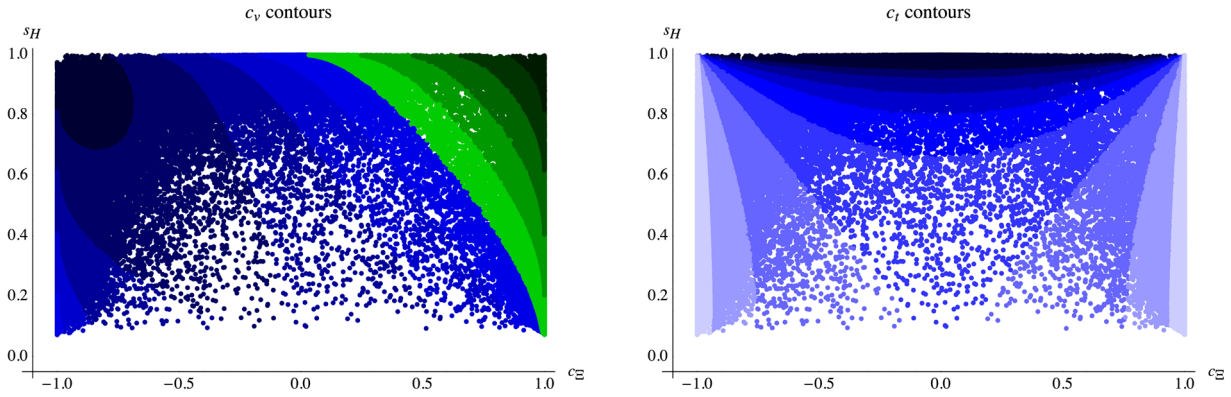

FIG. 8 (color online). Scan over the GM models parameter space only requiring $m_{H_0'} \simeq 126$ GeV in the (c_Ξ, s_H) plane. The left panel shows $c_{v,H_0'}$ contours with the following color codes: dark blue $-\sqrt{8/3} < c_v < -1.33$, dark green $1.33 < c_v < \sqrt{8/3}$. The right panel gives $c_{t,H_0'}$ contours with dark blue $c_t < -3$, light blue $-0.33 < c_t < 0$.

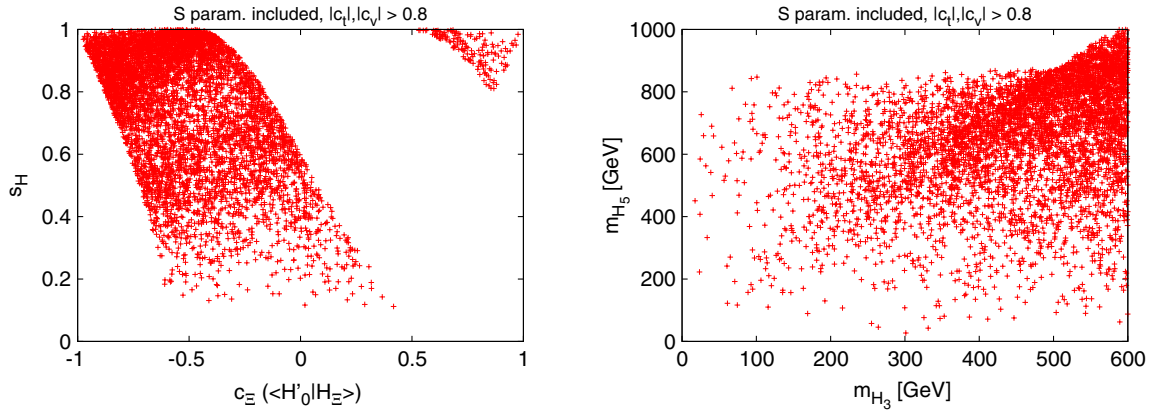

FIG. 9 (color online). Scan of Fig. 8, including precision constraints on the S parameter.

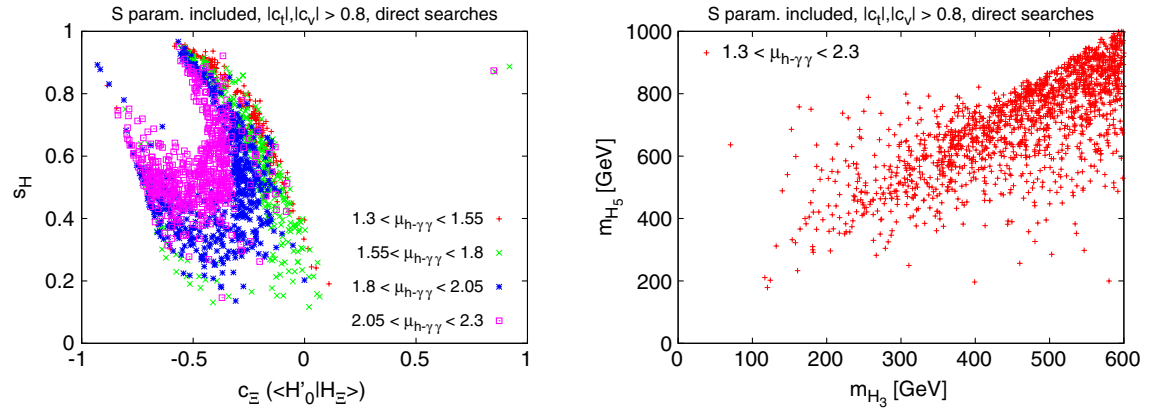

FIG. 10 (color online). Scan of Fig. 8, including precision constraints on the S parameter and signal strength constraints from direct searches.

to electroweak precision constraints: $|c_{v,H_0'}| \sim 1$ (vertical lines in Fig. 6) allows for a wide range on c_{v,H_0}.

Indeed, by enforcing electroweak precision constraints we find our results to be also less sensitive to the T parameter, although more parameter points at large s_H are rejected. Nonetheless we still obtain consistent parameter choice for large values of s_H, which as a consequence of signal strengths then needs to be anticorrelated to c_Ξ.

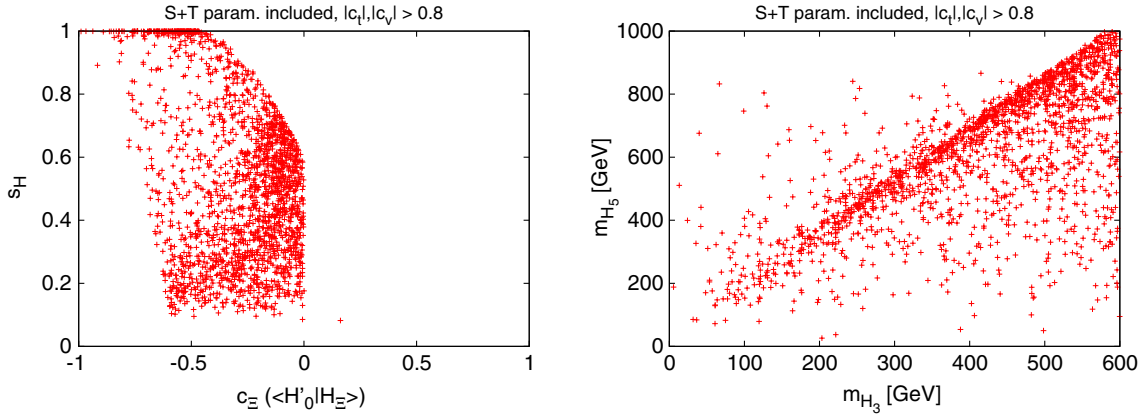

FIG. 11 (color online). Scan of Fig. 8, including precision constraints on both the S and the T parameters.

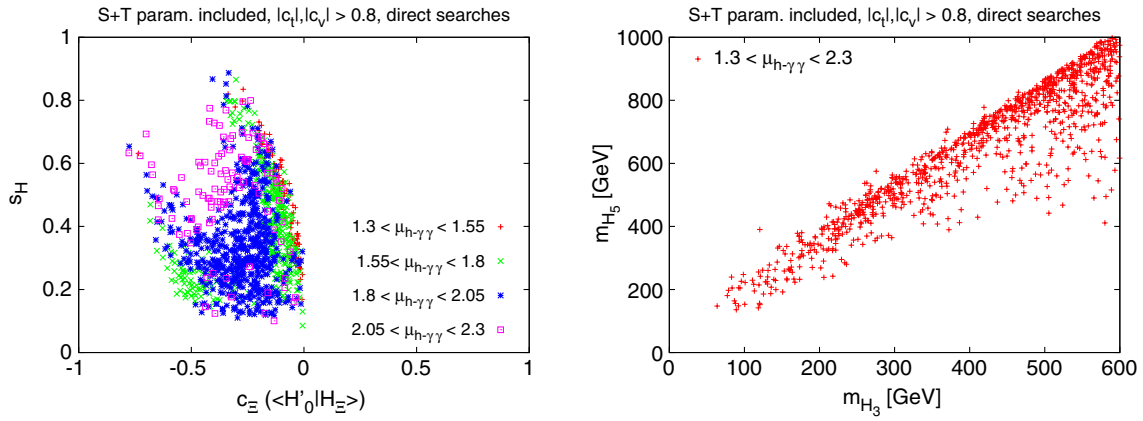

FIG. 12 (color online). Results of Fig. 10 including constraints on the S and T parameters, and signal strength constraints from direct searches.

The projection on (c_Ξ, s_H) therefore nicely discriminates between different regions of diphoton branching ratio enhancements. We again see that a potential excess in the diphoton final state in the GM model is predominantly realized via relaxing the SM constraints on couplings to the top and massive gauge boson sector with the additional scalars providing some additional freedom in this respect, yet their impact is subdominant unless m_{H_5} is significantly small.

A generic prediction of the GM model when it reproduces the current data and does not violate electroweak constraints on S, T is the presence of a relatively heavy quintet. The triplet states are also heavy but their phenomenology is sufficiently suppressed (keep in mind that we impose ATLAS exclusion contours on the uncharged states throughout). The quintet's production is suppressed but given the mass of this state we expect a measurement of the phenomenologically clean same-sign W production via WBF to give substantial constraints on the realization $m_{H_0'} \simeq 126$ GeV. Adapted searches will therefore have the potential to further constrain the GM model's allowed parameter space, or, conversely, to find a hint of a doubly charged scalar.

1. Heavy triplet—Light quintet

Until now our parameter choices are dominated by choices such that the quintet states typically outweigh the triplet Higgs bosons. Now, we specifically analyze the situation when the triplet is heavy ($m_{H,3} \simeq 500$ GeV) and the quintet states are light $m_{H_5} < m_{H_3}$. The resulting spectra with a heavy triplet and a relatively light quintet should be favored by flavor analyses, since the quintet is fermiophobic and the triplet is less related to fermion mass generation and should hence decouple for large masses from flavor observables, when s_H is not too large. We will also get a better understanding of the correlation between s_H and c_q.

As shown in Figs. 13 and 14, this dedicated scan projects out the values of $s_H \simeq 1$ with typically heavy additional singlets H_0 in the range of several 100 GeV. With respect to our previous remarks in Sec. IV B about how $H_0' \to \gamma\gamma$ comes about, we do not find any notable qualitative

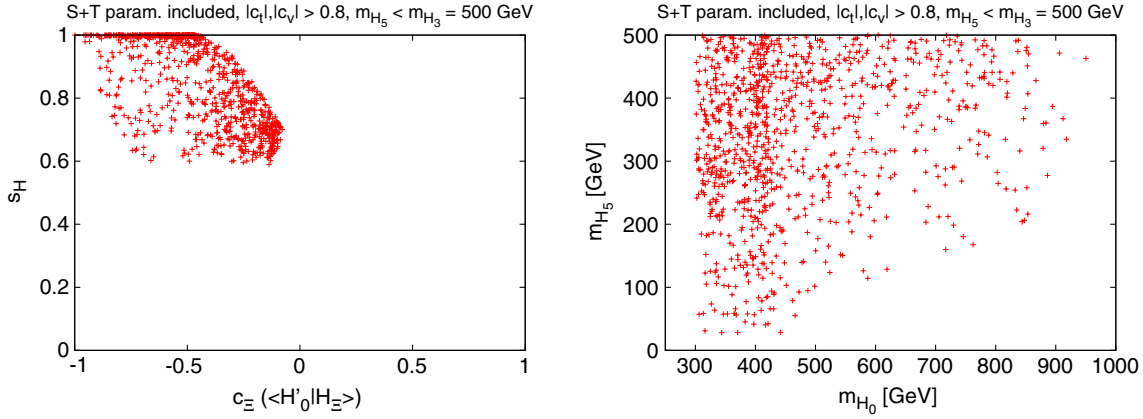

FIG. 13 (color online). Dedicated scan with $m_{H_3} = 500$ GeV and $m_{H_5} < m_{H_3}$ while $m_{H_0'} \simeq 126$ GeV. Constraints on both the S and T parameters are included.

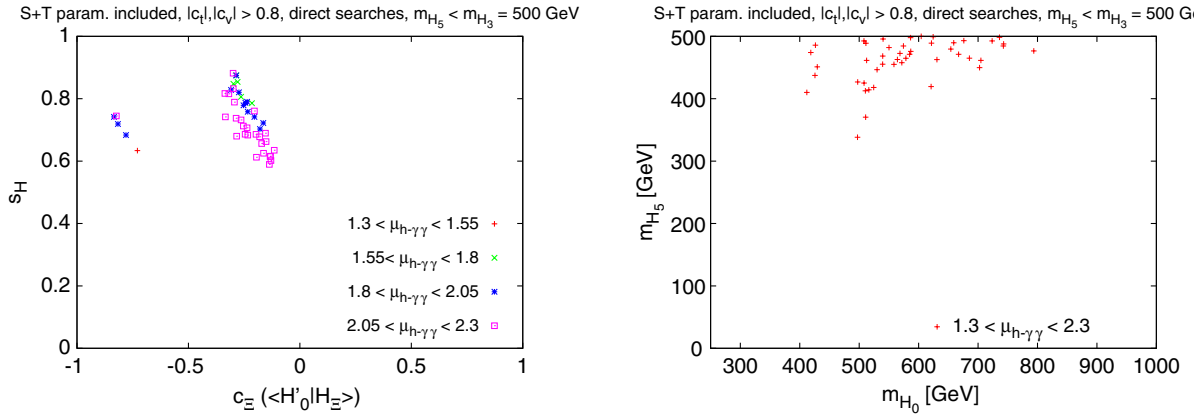

FIG. 14 (color online). Signal strengths included on top of the results of Fig. 13.

modification of our earlier findings: the enhanced diphoton branching is still predominantly enabled via the interplay of $c_{v,H_0'}$ and $c_{t,H_0'}$ and potentially large branching ratios can be achieved. These parameter choices typically imply a very large H_0 mass compared to the other case—future searches for uncharged SM Higgs-like states in the hundreds of GeV range will highly constrain this fact of the GM model.

2. SM-like GM phenomenology

Let us abandon the diphoton excess initially observed by both ATLAS and CMS and briefly investigate the parameter range for which $\mathrm{BR}(H_0' \to \gamma\gamma) \simeq \mathrm{BR}(h \to \gamma\gamma)_{\mathrm{SM}}$. This amounts to a potential future measurement which shows an even larger resemblance to the SM than we currently observe. Parameter choices of the GM model with such a measurement would be required to be more tailored to the SM. Identifying H_0 as our Higgs candidate is obviously still disfavored along the lines of our discussion of Sec. IV A. Furthermore, from our analysis of the $m_{H_0'} \simeq 126$ GeV it should be clear that the number of degrees of freedom in the light of not too constraining Higgs searches for masses different than 126 GeV and the available parameter space are large enough to account for such a situation (a limit of $\sigma \times \mathrm{Br}/[\sigma \times \mathrm{Br}]_{\mathrm{SM}} \simeq 0.1$ roughly corresponds to $|c_v| \lesssim 0.32$). This is especially true for parameter choices for which an additional scalar falls into the vicinity of the observed 126 GeV Higgs candidate, where resolution effects limit stringent constraints. We assume consistency with the SM hypothesis within 20% of the WW, ZZ, $\gamma\gamma$ and combined categories in the following, but we keep the ATLAS constraints on the other Higgs states unmodified. With our remarks about the (c_Ξ, s_H) plane being a good discriminant of the diphoton enhancement in mind we observe in Figs. 15 and 16 that the SM-like requirements slice out a specific parameter region in the GM model (independent of the T parameter).

This teaches two important lessons for an observation of perfectly consistent SM Higgs measurements in the future. On the one hand, even if such an outcome does not speak in favor of the GM model, there is still a lot of parameter space available, which can and needs to be tested at the LHC. From this point of view, it again appears

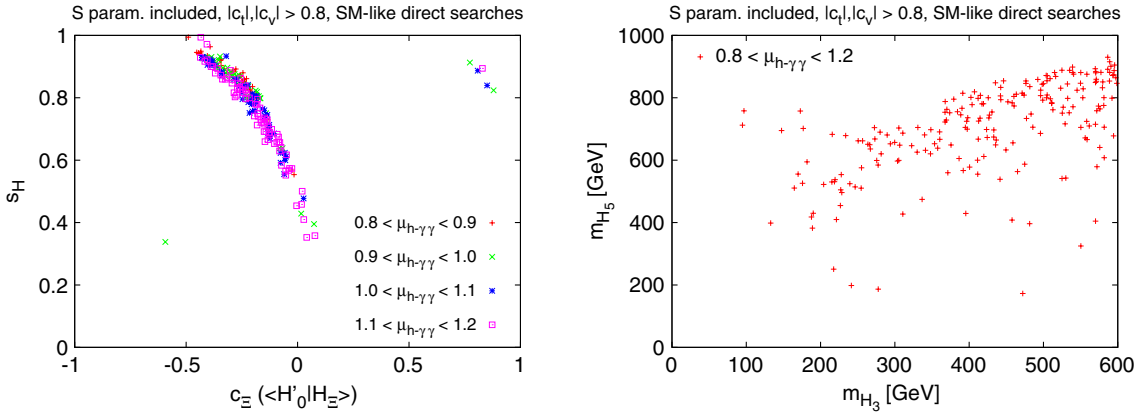

FIG. 15 (color online). Scan of Fig. 8, including precision constraints on the S parameter, and signal strength constraints, in a SM-like scenario where $\mu_{h\to WW}$, $\mu_{h\to\gamma\gamma}$ and the total μ value lie in the interval [0.8,1.2].

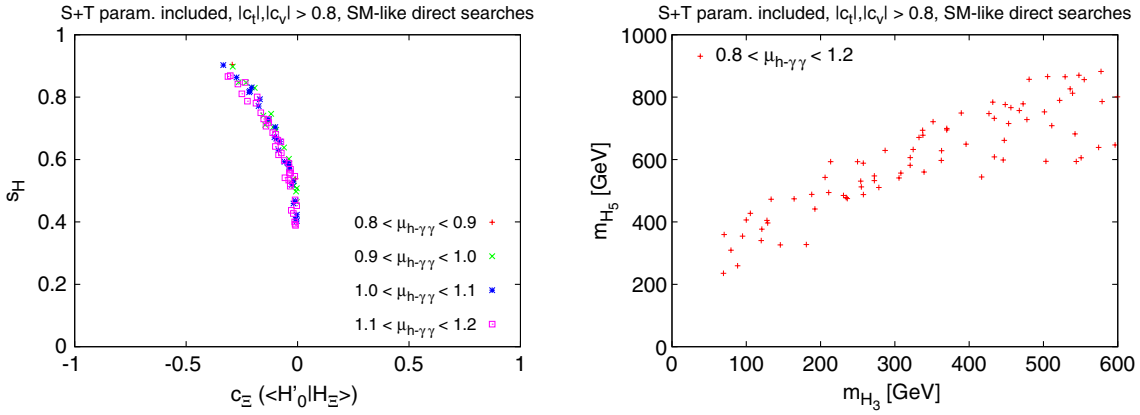

FIG. 16 (color online). Scan of Fig. 8, including precision constraints on the S and T parameters, and signal strength constraints, in a SM-like scenario where $\mu_{h\to WW}$, $\mu_{h\to\gamma\gamma}$ and the total μ value lie in the interval [0.8,1.2].

indispensable to extend existing Higgs-like searches to the heavy mass regime while relaxing specific assumptions on the total particle width as limiting factor of such analyses. With again quintet masses in the hundreds of GeV regime, which can be straightforwardly accessed at the LHC in same-sign W final states, the GM model can be highly constrained, even when its Higgs candidate phenomenology highly resembles the SM Higgs.

V. CONCLUSIONS

The Georgi-Machacek model implements Higgs triplets in a custodially invariant way at the price of an additional fine-tuning problem. In this paper we have performed an analysis of the model's parameter space in the light of direct collider and electroweak precision constraints. Depending on the interpretation of electroweak precision in the GM model context, there are important consequences for the model when it is confronted with data. Given that the GM model has a wide range of coupling spans, excesses in the $h \to \gamma\gamma$ rate can be observed, but there is also a vast parameter region that is allowed if data resembles the SM.

In addition to the SM, the GM model introduces a number of new scalars. However, in the light of recent measurements only a subset of these can be considered the discovered Higgs candidate. One peculiarity that arises in the GM model is that if the Higgs boson that arises mostly from the SM-like doublet Higgs field is identified with the Higgs candidate at around 126 GeV, there is a light scalar in the spectrum which mostly arises from the triplet. This puts strong constraints on this option as branching ratios to SM matter quickly deviate from their observed values when the light scalar becomes accessible as a Higgs decay channel. Furthermore, electroweak precision constraints (mostly by the S parameter) disfavor this option even if the light scalar is not constrained by LEP measurements. If the excess in the diphoton channel prevails this option becomes heavily constrained whereas lower combined signal strengths can be obtained at the cost of a tension with electroweak precision data.

Most of these constraints are relaxed when we identify the nondoublet state with the observed candidate. Here a vast parameter space becomes available to accommodate excesses in the $\gamma\gamma$ channel, but the model also exhibits parameter regions consistent with SM.

For our simplified Lagrangian approach, the consistent parameter choices of the SM typically predict the presence of new states in the hundreds of GeV region. Lighter spectra are admissible by current collider constraints but typically result from extremely small mixing of the custodial triplets, one of which giving rise to massive gauge bosons. While the triplet mass eigenstate is $\mathcal{CP}$ odd and can only be produced via gluon fusion, the quintet state is fermiophobic and can be constrained via a dedicated measurement in WBF-type production in the near future. The latter search is likely to put extremely tight constraints on the GM model, especially if future measurements of the 126 GeV Higgs candidate are consistent with the SM predictions.

ACKNOWLEDGMENTS

We would like to thank Claude Duhr for FEYNRULES support. C. E. thanks Adam Falkowski and Jure Zupan for discussions during the CERN BSM Theory Summer Institute. E. R. thanks Uli Haisch for useful discussions. C. E. acknowledges funding by the Durham International Junior Research Fellowship scheme.

[1] F. Englert and R. Brout, Phys. Rev. Lett. **13**, 321 (1964); P. W. Higgs, Phys. Lett. **12**, 132 (1964); Phys. Rev. Lett. **13**, 508 (1964); G. S. Guralnik, C. R. Hagen, and T. W. B. Kibble, Phys. Rev. Lett. **13**, 585 (1964).
[2] ATLAS Collaboration, Phys. Lett. B **716**, 1 (2012).
[3] CMS Collaboration, Phys. Lett. B **716**, 30 (2012).
[4] ATLAS Collaboration, Report No. ATLAS-CONF-2012-170.
[5] CMS Collaboration, Report No. CMS-PAS-HIG-12-045.
[6] S. Chang, C. A. Newby, N. Raj, and C. Wanotayaroj, Phys. Rev. D **86**, 095015 (2012).
[7] A. G. Akeroyd and S. Moretti, Phys. Rev. D **86**, 035015 (2012).
[8] D. Carmi, A. Falkowski, E. Kuflik, T. Volansky, and J. Zupan, J. High Energy Phys. 10 (2012) 196.
[9] M. E. Peskin and T. Takeuchi, Phys. Rev. Lett. **65**, 964 (1990); Phys. Rev. D **46**, 381 (1992).
[10] H. Georgi and M. Machacek, Nucl. Phys. **B262**, 463 (1985); M. S. Chanowitz and M. Golden, Phys. Lett. **165B**, 105 (1985).
[11] K. Cheung and D. K. Ghosh, J. High Energy Phys. 11 (2002) 048.
[12] S. Godfrey and K. Moats, Phys. Rev. D **81**, 075026 (2010).
[13] M. Chaichian, P. Hoyer, K. Huitu, V. A. Khoze, and A. D. Pilkington, J. High Energy Phys. 05 (2009) 011.
[14] L. Wang and X.-F. Han, Phys. Rev. D **86**, 095007 (2012); **87**, 015015 (2013).
[15] H. E. Logan and M.-A. Roy, Phys. Rev. D **82**, 115011 (2010).
[16] J. F. Gunion, R. Vega, and J. Wudka, Phys. Rev. D **42**, 1673 (1990).
[17] A. Djouadi, W. Kilian, M. Mühlleitner, and P. M. Zerwas, Eur. Phys. J. C **10**, 27 (1999); U. Baur, T. Plehn, and D. L. Rainwater, Phys. Rev. D **69**, 053004 (2004); M. J. Dolan, C. Englert, and M. Spannowsky, J. High Energy Phys. 10 (2012) 112; F. Goertz, A. Papaefstathiou, L. L. Yang, and J. Zurita, arXiv:1301.3492.
[18] G. 't Hooft, NATO ASI Ser., Ser. B **59**, 135 (1980).
[19] A. Arhrib, R. Benbrik, M. Chabab, G. Moultaka, and L. Rahili, J. High Energy Phys. 04 (2012) 136.
[20] N. D. Christensen and C. Duhr, Comput. Phys. Commun. **180**, 1614 (2009).
[21] A. G. Akeroyd, Phys. Lett. B **353**, 519 (1995).
[22] J. F. Gunion, P. Kalyniak, M. Soldate, and P. Galison, Phys. Rev. Lett. **54**, 1226 (1985).
[23] J. F. Gunion, R. Vega, and J. Wudka, Phys. Rev. D **43**, 2322 (1991).
[24] C. Wetterich, Phys. Lett. **140B**, 215 (1984).
[25] R. Barbieri, A. Pomarol, R. Rattazzi, and A. Strumia, Nucl. Phys. **B703**, 127 (2004).
[26] V. D. Barger, J. L. Hewett, and R. J. N. Phillips, Phys. Rev. D **41**, 3421 (1990); J. F. Gunion and H. E. Haber, Phys. Rev. D **67**, 075019 (2003).
[27] H. E. Haber and H. E. Logan, Phys. Rev. D **62**, 015011 (2000).
[28] CMS Collaboration, Eur. Phys. J. C **72**, 2189 (2012); ATLAS Collaboration, Eur. Phys. J. C **72**, 2244 (2012).
[29] CMS Collaboration, Phys. Rev. Lett. **109**, 071803 (2012); CMS Collaboration, Report No. CMS-PAS-SUS-12-017; ATLAS Collaboration, J. High Energy Phys. 10 (2011) 107.
[30] D. Goncalves-Netto, D. Lopez-Val, K. Mawatari, T. Plehn, and I. Wigmore, Phys. Rev. D **87**, 014002 (2013).
[31] A. G. Akeroyd, M. Aoki, and H. Sugiyama, Phys. Rev. D **79**, 113010 (2009).
[32] M. Kakizaki, Y. Ogura, and F. Shima, Phys. Lett. B **566**, 210 (2003).
[33] W. Konetschny and W. Kummer, Phys. Lett. **70B**, 433 (1977).
[34] CMS Collaboration, Report No. HIG-12-041.
[35] H. M. Georgi, S. L. Glashow, M. E. Machacek, and D. V. Nanopoulos, Phys. Rev. Lett. **40**, 692 (1978); A. Djouadi, M. Spira, and P. M. Zerwas, Phys. Lett. B **264**, 440 (1991); S. Dawson, Nucl. Phys. **B359**, 283 (1991); M. Spira, A. Djouadi, D. Graudenz, and P. M. Zerwas, Nucl. Phys. **B453**, 17 (1995); R. V. Harlander and W. B. Kilgore, Phys. Rev. Lett. **88**, 201801 (2002); S. Moch and A. Vogt, Phys. Lett. B **631**, 48 (2005).

[36] D. L. Rainwater and D. Zeppenfeld, J. High Energy Phys. 12 (1997) 005; D. L. Rainwater, D. Zeppenfeld, and K. Hagiwara, Phys. Rev. D **59**, 014037 (1998); T. Figy, D. Zeppenfeld, and C. Oleari, Phys. Rev. D **68**, 073005 (2003); for electroweak corrections in the context of the SM electroweak sector, see M. Ciccolini, A. Denner, and S. Dittmaier, Phys. Rev. Lett. **99**, 161803 (2007).

[37] S. Dittmaier *et al.* (LHC Higgs Cross Section Working Group Collaboration), arXiv:1101.0593.

[38] ATLAS Collaboration, Report No. ATLAS-CONF-2012-127.

[39] R. Barate *et al.* (LEP Working Group for Higgs boson searches and ALEPH, DELPHI, L3 and OPAL Collabs), Phys. Lett. B **565**, 61 (2003).

[40] CMS Collaboration, Report No. CMS-HIG-12-045; ATLAS Collaboration, Report No. ATLAS-CONF-2012-127.

[41] A. Azatov, R. Contino, and J. Galloway, J. High Energy Phys. 04 (2012) 127; P. P. Giardino, K. Kannike, M. Raidal, and A. Strumia, Phys. Lett. B 718, 469 (2012); J. Ellis and T. You, J. High Energy Phys. 09 (2012) 123; J. R. Espinosa, C. Grojean, M. Muhlleitner, and M. Trott, J. High Energy Phys. 12 (2012) 045; T. Plehn and M. Rauch, Europhys. Lett. **100**, 11002 (2012); G. Moreau, Phys. Rev. D **87**, 015027 (2013); T. Corbett, O. J. P. Eboli, J. Gonzalez-Fraile, and M. C. Gonzalez-Garcia, Phys. Rev. D **87**, 015022 (2013); E. Masso and V. Sanz, Phys. Rev. D **87**, 033001 (2013).

[42] P. Meade and M. Reece, arXiv:hep-ph/0703031.

[43] A. Djouadi, Phys. Rep. **457**, 1 (2008).

[44] S. Alioli, P. Nason, C. Oleari, and E. Re, J. High Energy Phys. 04 (2009) 002; 06 (2010) 043.

[45] J. Alcaraz *et al.* (ALEPH and DELPHI and L3 and OPAL and LEP Electroweak Working Group Collaborations), arXiv:hep-ex/0612034.

[46] M. Baak, M. Goebel, J. Haller, A. Hoecker, D. Kennedy, R. KoglerK. Mönig, M. Schott, and J. Stelzer, Eur. Phys. J. C **72**, 2205 (2012).